Improving the Illumination Uniformity of a Cryogenic Target with a Layering Sphere

Brian Way Pan
Penfield High School
Penfield, NY 14526

Advisor: Dr. Wolf Seka
Laboratory for Laser Energetics
University of Rochester
250 East River Road
Rochester, NY 14623

*August 24, 2005**

Abstract

One of the considerations in creating a precisely layered cryogenic target requires uniform heating due to uniform illumination of the target by an infrared (IR) laser shined within the layering sphere, which has an inner, gold-coated rough metal surface. The layering sphere was originally thought to have Lambertian scattering characteristics that result in uniform heating. However, measurements have shown that the surface scattering characteristics of the layering sphere are far from Lambertian. Using a periscope setup at the location of the cryogenic target at the center of the layering sphere, the illumination uniformity (or lack thereof) was evaluated. A wide-angle diffuser configuration placed at the input of the heating laser demonstrates a significant improvement of the illumination uniformity that closely resembles the illumination uniformity achieved in a perfect integrating sphere. Finally, the periscope results were analyzed to determine the effect of the keyhole and four viewing windows of the layering sphere on the illumination uniformity of the target.

* This work was presented on August 24, 2005, 2005 Summer High School Student Research Symposium, LLE Coliseum.

1. Introduction

In the direct-drive inertial confinement fusion (ICF)[1] concept, a cryogenic spherical capsule containing thermonuclear fuel is imploded by 60 laser beams, which are directed on the surface of the capsule in a nearly uniform pattern. Much of the current ICF research uses the 60-beam, 30-kJ UV OMEGA laser system[2] at the Laboratory of Laser Energetics (LLE) of the University of Rochester. The research is performed to understand the requirements and determine the conditions for a high energy yield from fusion reactions so that ignition of deuterium-tritium fuel may be demonstrated at the National Ignition Facility (NIF) at Lawrence Livermore National Laboratory (LLNL) in the near future.

1.1 Cryogenic Target

The OMEGA cryogenic target design (Fig. 1) is a 0.9-mm spherical plastic shell with a 5-μm plastic shell (CH). This target is filled with D_2 at 1500 atm, cooled to cryogenic temperatures, and located at the center of a 2.5-cm diameter layering sphere[3] (Fig. 2b). This gas density equates to a frozen deuterium wall thickness of approximately 100 μm, thereby delivering a high concentration of fusion fuel.

1.2 Layering Sphere and Process

One of the processes for creating a deuterium solid layer starts with the target below the triple point (18.72 ^{o}K) and with a frozen lump of deuterium ice in the bottom of the target[3]. Deuterium is then layered by uniformly bathing and heating the target in infrared (IR) radiation. This process causes the deuterium ice to become warmer than the plastic shell's surface. The solid deuterium sublimes from where it is thickest and re-condenses where it is thinnest because the IR light (wavelength, $\lambda = 3.16\mu m$[3]) is preferentially absorbed by the deuterium ice. With appropriate controls on the temperature of the layering sphere and the heating laser, the thickness

of the ice wall is expected to become uniform. In practice, however, the resulting ice layer is not uniform. Three-dimensional (3-D) characterization of the ice layer using optical shadowgraphy[3,4] has shown peak-to-valley variations of ≤ 20 μm (Fig. 2a) in the ice layer thickness.[3,5] The ice layer thickness variation and other layer imperfections[6] such as craters and cracks typically result in significant degradation of fusion yield in implosion experiments.

Currently, the layering sphere has obvious imperfections that may affect the IR illumination uniformity on the target. The inner surface of the layering sphere is roughened, gold-coated metal. In reflecting an incoming light beam off the inner surface and about the surface normal, a specular lobe in the specular direction is produced. The first and second reflections are more significant. Later, they will be referred to as "bright spots." Other imperfections of the layering sphere are due to the "windows" and "keyhole" (Fig. 2b). It is important to assess the effect of these unavoidable holes in the layering sphere for viewing target and target insertion.

1.3 Project Goal

It is important that LLE produces targets with uniform ice layer. A uniform cryogenically frozen deuterium ice layer within a 1-mm sized plastic capsule should be created inside a layering sphere. The layering sphere has provisions to inject a heating laser through an optical fiber that causes unevenly frozen deuterium to redeposit the D_2 ice uniformly. Uniform illumination of the target by the heating laser is expected to generate even deposition of deuterium all around the plastic capsule. The scattering characteristics of the heating laser light, within the layering sphere, were not known. So, the goal is to first determine the heating illumination uniformity (or lack thereof) at the center of the layering sphere. Then, comparing the uniformity of that sphere to the uniformity of a perfect integrating sphere, we were to analyze

root causes of non-uniform illumination. Finally, we wanted to propose a solution for creating more uniform heating illumination in the sphere to attain uniform D_2 targets.

The motivation for improving the scattering characteristics of the layering sphere is the possibility of generating more uniform targets, which could, in turn, lead to more effective target implosions and more net energy gain in the fusion reactions. Such improvements would also benefit other facilities such as NIF at LLNL.

2. Experimental

To establish the illumination pattern of the center of the layering sphere and to compare it with the illumination pattern within a perfect integrating sphere, an apparatus, as shown in Fig. 3, was set up using a visible light emitting diode (LED) around 630 nm to replace the IR heating laser. This "periscope" would mimic what the cryogenic target experiences in one plane at a time. The periscope consisted of a 0.5 mm optical fiber with a small glass prism optically coupled to the end of the fiber; the periscope was then rotated within the layering sphere using a computer controlled motor. The optical fiber piped the light collected by the prism to a photodiode whose output was displayed on an oscilloscope and subsequently, on a computer.

Because reproducibility in a wide variety of setups was essential, computer-controlled rotation and data acquisition was implemented. Reproducibility of the data was assured by taking at least 3 scans for each experimental setup. Data were then displayed in either polar or rectangular coordinates as oscilloscope readings *versus* angle of rotation (motor position).

Illumination uniformity data were acquired for equatorial views of a perfect integrating sphere and an actual layering sphere, along with a tilted-plane view of the layering sphere. The equatorial views included views of the windows (partial views in some cases). The tilted-plane

view included a significant part of the keyhole area. Then, equatorial and tilted-plane views of the proposed solution were taken.

3. Results and Discussion

The layering sphere is designed to work with the LLE's Cryogenic Target Handling System[7], so only absolutely necessary modifications to the sphere can be carried out. Additionally, it is important to note that the sphere's inner surface itself is roughened gold, which can tolerate the cold temperatures and high acceleration, which the surface, just prior to a laser fusion shot, is exposed to. The sphere also reflects the 3.16 μm heating IR laser better than most other surface treatments.

3.1 Current Illumination Uniformity Level

Using the periscope we can quantify the current illumination non-uniformity inside the layering sphere in two planes, the equatorial view and a tilted plane. We also compared these data with data collected from a "perfect" integrating sphere whose surface was a known Lambertian[9] scatterer.

Typical plots of equatorial scan data for the layering sphere are shown in Fig. 4 in which the scope readings (mV) were normalized to the maximum reading and plotted *vs.* angle of periscope rotation (degree). Figure 4a is a polar plot of the data while Fig. 4b is the equivalent Cartesian plot. The polar plot depicts the angular non-uniformities in a more qualitative way while the Cartesian plot is more convenient for quantitative interpretation.

The layering sphere with all windows closed shows two maxima and two minima in Fig. 4 (red curves). The intensity fluctuation between maximum and minimum is >2. Further observation of the data in Fig. 4 suggests that the maxima can be attributed to the first and

second bounces of the semi-specular reflections. These "bright spots," would be even brighter if the equatorial scan were to view the entire area of the first or second bounces.

3.2 Uniformity Goal: Lambertian Integrating Sphere

In order to establish an illumination standard for comparison with the data obtained from the layering sphere, an integrating sphere with "Lambertian" scattering[8] characteristics was investigated using the same periscope arrangement. The inner surface of the sphere is a white, powdery surface whose scattering characteristics were measured using a witness piece and was found to closely follow the Lambert's cosine law (Fig. 5).

Plots of equatorial scan data for the perfect integrating sphere are shown in blue curves in Fig. 4. The illumination uniformity at the center of this sphere was significantly better than the results obtained from the layering sphere. There are no noticeable bright spots and the overall fluctuations in trace do not exceed ±10%. It should be noted that integrating spheres are usually used as uniform sources for light exiting through a small hole in the sphere. Uniformity of illumination at the center of the integrating sphere is a non-standard application that does not necessarily lead to perfect uniformity. Thus this experiment by itself demonstrated an important point, i.e. that a good integrating sphere indeed leads to quite tolerable illumination uniformity at the center of the sphere.

3.3 Scattering Characteristics of the Inner Layering Sphere Surface

Figure 4 clearly demonstrates the difference in the illumination uniformity between the layering sphere and the perfect Lambertian integrating sphere. This difference mainly results from the non-Lambertian, semi-specular characteristics of the inner surface of the layering sphere. The detailed scattering characteristics of the inner surface of the layering sphere have been measured separately and are shown in Fig.5.

The scattering characteristics of a gold-coated rough metal witness plate, which is similar to that of the inner surface of the layering sphere, was determined by M. Alexander et al.[9] The reflected intensity was measured as a function of detection angle by shining an incident laser beam at 135^o incident angle. The measured reflected intensity was normalized to the maximum intensity value and plotted as a function of viewing angle (red triangles) in Fig. 5. The normalized reflected intensity distribution was also calculated[4] using the equation (1) and displayed (red dash curve) in Fig. 5:

$$R = k\, R_L \cos^n(\theta-\theta_0) \qquad (1)$$

In this equation, θ = viewing angle, θ_0 = specular reflection angle (=45^o), n=9 (best fit the data[4)], k is the normalization constant such that maximum R is equal to 1, and R_L in equation (1) is the Lambertian intensity distribution[8]:

$$R_L = \cos(90^o - \theta) \qquad (2)$$

This is also shown (green solid curve) in Fig. 5. The measured results (green squares) are in agreement with the Lambert's cosine law. The data in Fig.5 point out the non-ideal scattering properties of the gold-coated rough surface of the layering sphere as one of the root causes to the non-uniform illumination problem.

3.4 Uniformity Improvement by a Wide-Angle Diffuser Configuration

There are two obvious solutions to increase the illumination uniformity of the layering sphere at its center: (1) placing diffusers into the laser beam that spread the area of the first bounce, and (2) making the surface Lambertian-like. Solution 2 is difficult to implement because of absorption problems in the 3-μm wavelength range, the cold temperatures and the high acceleration (5 to 7g) that the sphere experiences just prior to the laser shot. Solution 1 was therefore pursued further.

The layering sphere was insignificantly modified to incorporate the use of a very small, eighty-degree wide-angle diffuser, as shown schematically in Fig. 6. The diffuser is an "engineered" diffuser that scatters the light in the forward direction into an 80-degree cone with over 90% efficiency. The diffuser was mounted such that its plane went "through" the center of the target and thus minimized any light scattered directly by the diffuser from reaching the target. Any other arrangements appear to lead to less desirable illumination uniformities at the center of the sphere.

Direct illumination of the target by the diffuser was further minimized by placing another small diffuser on top of the primary diffuser as shown in Fig. 6. The first bounce area on the layering sphere was thus significantly enlarged and the illumination non-uniformity at the center of the sphere was significantly improved and approached that of the perfect integrating sphere.

Equatorial scans of the modified layering sphere are shown in red curves (dash) in Fig. 7 along with corresponding data obtained with the unmodified layering sphere (red, solid) and the perfect integrating sphere (blue, dash-dot). The improved illumination uniformity obtained with the modified layering sphere is obvious and compares favorably with the data obtained for the perfect integrating sphere.

The ratio of peak-to-valley variations in intensity can be used to quantify the illumination uniformity (1 = perfect uniformity). The intensity ratio for the original layering sphere, the modified layering sphere, and the perfect integrating sphere are 2.78, 1.52, and 1.32, respectively. A vast improvement thus resulted from the implementation of a wide-angle diffuser. Of course, these data were taken for equatorial views with all windows closed and keyhole outside the scan.

3.5 Effect of Open Windows

The layering sphere has two pairs of opposing sapphire windows (~6-mm diameter) oriented along axes corresponding to the viewing axes in the OMEGA target chamber. The windows corresponding to the X- and Y-axis views are positioned 26.6^{o} and 12^{o} above and below the equator, respectively, and 110^{o} apart. Thus it is possible to detect the impact of opening the windows on illumination uniformity by the equatorial scan.

Figure 8 shows the effect on intensities that demonstrates the lack of scattered light from the regions of the open windows. We note that the intensity curves are nearly identical for open and closed windows except for one significant valley area at about 120^{o}. A secondary dip near 20^{o} is less pronounced. The difference in the perturbations caused supposedly by the two sets of two windows is due to the angular offset of the windows (12^{o} and 26.6^{o}). It is believed that the 12^{o} windows are almost completely covered by the equatorial view while the 26.6^{o} windows are only partially seen. In principle, two large perturbations due to the 12^{o} windows and two small perturbations due to the 26.6^{o} windows should be observed. On the contrary, only one large perturbation and one small perturbation were notable in Fig. 8. The 100^{o} separation between the intensity valleys is very close to the actual azimuthal angular offset of the 26.6^{o} and 12^{o} window locations. No significant perturbations due to the other 26.6^{o} and 12^{o} windows were observed in Fig. 8. One of the possible explanations for this discrepancy is that the periscope was not properly positioned and the "equatorial" scan was actually biased in one direction. In light of this, we feel that this conclusion is still valid: windows cause perturbations on the illumination uniformity.

3.6 Effect of Keyhole

In order to investigate the effect of the keyhole on the illumination uniformity at the center of the sphere, a tilted-plane scan of the layering sphere was established. The periscope is

inserted through one of the windows of the layering sphere (Fig. 9). This scan permits a partial view of the keyhole, a complete view of the window through which the periscope was positioned, and a small view of the opposite window with angular offset of approximately 24^{o}.

Figure 10 shows the effect of the keyhole on the uniformity perturbation in the tilted-plane view with all windows open. The dash and solid curves were acquired from the original and the modified layering sphere. There are two significant intensity valleys in both cases. One at about 160^{o} is attributed to the keyhole and the other at about $30\text{-}40^{o}$ is due to one of the open window through which the periscope was positioned. The keyhole causes much more significant perturbation of intensity on the target over a wider range of angle than any other factors.

Although the area of the entry keyhole is 2% to 3% of the total area, the results (Fig. 10) indicate that it is the single, most profound feature affecting illumination uniformity. The only way to ameliorate the conditions is to simply reduce its size. In addition, the tilted view does not see the complete effect of the keyhole—the perturbation is expected to be even worse.

3.7 Illumination Uniformity Factor

The illumination uniformity factor, ε is defined as the ratio of peak (maximum) to valley (minimum) intensity, as described in Section 3.4. The ε value of perfect illumination uniformity is equal to one (unity); the higher the ratio value, the greater the deviation of peak. Table I summarizes the illumination uniformity factor versus various experimental settings (column 2-6).

Table I. Illumination uniformity factor quantifying the improvement due to the optimal wide-angle diffuser configuration and various effects.

	Main setting	Modifications	Windows	Scan type	Feature scanned	Uniformity Factor, ε
Goal	Perfect integrating sphere	None	None	Equatorial	None	1.32
1	Original layering sphere	Initial design	Closed	Equatorial	None	2.78
2	Original layering sphere	Initial design	Open	Equatorial	Windows	4.08
3	Original layering sphere	Initial design	Open	Tilted	Keyhole	6.25
4	Modified layering sphere	Wide-angle diffuser	Closed	Equatorial	None	1.52
5	Modified layering sphere	Wide-angle diffuser	Open	Equatorial	Windows	1.89
6	Modified layering sphere	Wide-angle diffuser	Open	Tilted	Keyhole	4.17

The illumination uniformity factor is also plotted in Fig. 11 to better illustrate that the layering sphere modified with a wide-angle diffuser improves the illumination uniformity in all cases, as compared to the original layering sphere under the same experimental settings.

4. Summary and Recommended Future Work

The results in Table I and Fig. 11 have already demonstrated a significant improvement in illumination uniformity from the layering sphere with a wide-angle diffuser configuration, but future work using a computer-controlled movement of the periscope (or a miniature CCD/IR camera) along the axis perpendicular to the equatorial plane and to the tilted plane for the collection of views over almost the entire layering sphere is suggested. The data can be stitched together to provide a 3-D illumination map. This map can then be quantitatively correlated region by region with an ice layer thickness variation map. The quantitative contribution of the keyhole, blind spot[4] and other imperfections in the layering sphere to the ice layer thickness variation can be evaluated. Furthermore, the upper limit of the illumination factor can then be set.

Other future work is also recommended to better understand the effect of the diffuser on the thermal environment of the target since a temperature gradient of a few hundredths of a degree in the layering sphere can cause a significant variation in the ice layer thickness.[10] The engineered diffuser used in the modified layering sphere needs to have very low absorption at 3.16 μm, which we have not measured in these experiments. Another solution would have to be found to spread the input beam if the absorption were significant. The experiment using the diffusers should also be performed using the real fiber-coupled heating IR laser instead of the surrogate LED red light.

New problems may be posed by all these tasks. However, the prospects and principles of better uniformity due to wide-angle light distribution remain highly promising.

5. Conclusion

The original layering sphere was found to have poor illumination uniformity due to scattering properties of the inner surface. The first two bounces of the heating laser cause significant bright spots. We have improved the target illumination uniformity inside the layering sphere due to the first and second bounce bright spots of the heating laser. In contrast, a perfect integrating sphere does not show these bright spots. The bright spots were identified to be due to the non-Lambertian scattering characteristics of the layering sphere. Insertion of a wide-angle engineered diffuser improved the illumination uniformity almost to the level of the perfect integrating sphere, because the first bounce illumination area was greatly increased. Unfortunately it was confirmed that the presence of the large keyhole and four windows in the layering sphere cause very significant illumination non-uniformities.

6. Acknowledgements

First and foremost, I would like to thank my advisor, Dr. Wolf Seka, for his time and effort in helping me with this project. I am also grateful to Dr. R. Stephen Craxton for giving me the opportunity to be a part of the 2005 Summer High School Research Program. I would like to thank my fellow comrades at the LLE who were in the program with me, for their continual support. Also, I need to thank both Michelle and Josh for their help with the MATLAB programs and professional yet friendly presence in the lab. The photos Eugene Kowaluk took that are used in this presentation were astounding, thank you for your help as well. Lastly, I would like to thank my family for their support and help, all along the way.

7. References

***** This report is based on the work at the LLE Summer High School Student Research Program, July 5 - August 29, 2005.

1. J. Nuckolls et al., Nature, 239, 139 (1972).
2. T.R.Boehly, D.L. Brown, R.S. Craxton, R.L. Keck, J.P. Knauer, J.H. Kelly, T.J. Kessler, S.A. Kumpan, S.J. Loucks, S.J. Letzring, F.J. Marshall, R.L. McCrory, S.F. B. Morse, W. Seka, J.M. Sources and C.P. Verdon, Opt. Commun., 133, 495 (1997).
3. LLE Review, "Formation of Deuterium-Ice layers in OMEGA Targets", 99, 160 (2003)
4. D.E. Edgell, "Three-Dimension Characterization of Ice Layers for Cryogenic Targets at LLE", Presented at the 46th Annual Meeting of the American Physical Society, Division of Plasma Physics, Savannah, GA, November 15-19, 2004.
5. D.R. Harding, M.D. Wittman, L.M. Elasky, S. Verbridge, L.D. Lund, D. Jacobs-Perkins, W. Seka, D.H. Edgell, and D.D. Meyerhofer, "OMEGA Direct-Drive Cryogenic Deuterium Targets," Presented at the 46th Annual Meeting of the American Physical Society, Division of Plasma Physics, Savannah, GA, November 15-10, 2004.
6. L. Weiss, "Categorization and Analysis of Defects in Cryogenic Targets", Presented at the 2005 Summer High School Student Research Program Symposium, Laboratory for Laser Energetics Coliseum, August 24, 2005.
7. LLE Review, "Initial Performance of the High Pressure DT-Filling Portion of the Cryogenic Target Handling System", 81, 6 (1999).

8. A Lambertian surface is a surface of perfectly matte properties, which means that it adheres to *Lamberts cosine law*. Lamberts cosine law states that the reflected or transmitted *luminous intensity* in any direction from an element of a perfectly diffusing surface varies as the cosine of the angle between that direction and the *normal vector* of the surface. As a consequence, the *luminance* of that surface is the same regardless of the viewing angle.
9. M. Alexander et al., Reflected luminous intensity data taken from a typical gold-coated rough surface, LLE, August 2004.
10. D.R. Harding, "Forming Smooth Cryogenic Targets for OMEGA Direct-Drive ICF Implosions and Prospects for Direct-Drive Targets for the NIF, Presented at the 47th Annual Meeting of the American Physical Society Division of Plasma Physics, Denver, CO, October 24-28, 2005.

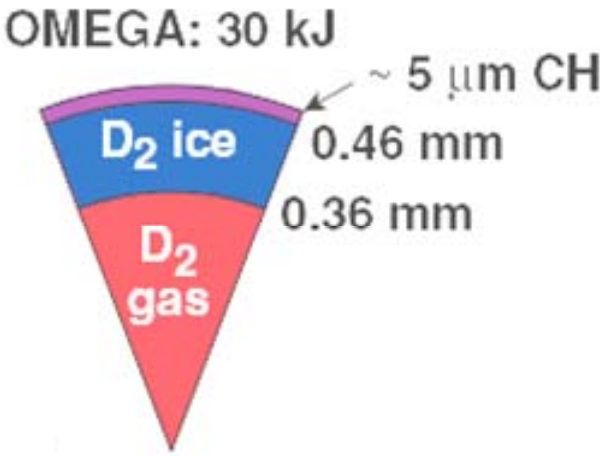

Fig. 1 Cross sections of OMEGA direct-drive targets, showing target component layers and their dimensions. Purple: CH for a thin plastic shell. Blue: cryogenically frozen D_2 layer.

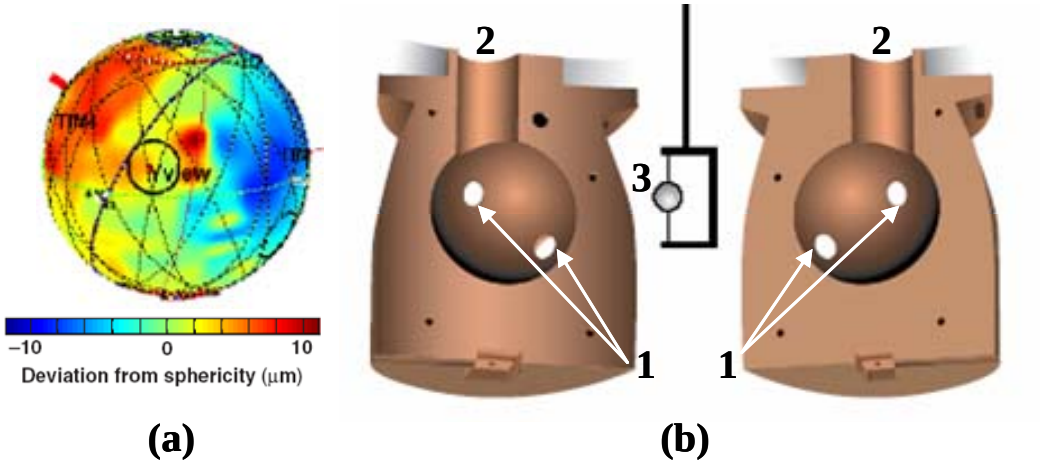

Fig. 2 (a) A 3-D plot of deuterium ice layer thickness using optical shadowgraphy shows ice layer thickness deviation.[5] (b) The layering sphere, shown in two hemispheres side by side, has (1) two pairs of opposing windows. The (2) "keyhole" opening at the base of the layering sphere is where the (3) target, mounted on four web of spider silks supported by a hook, is inserted and removed.

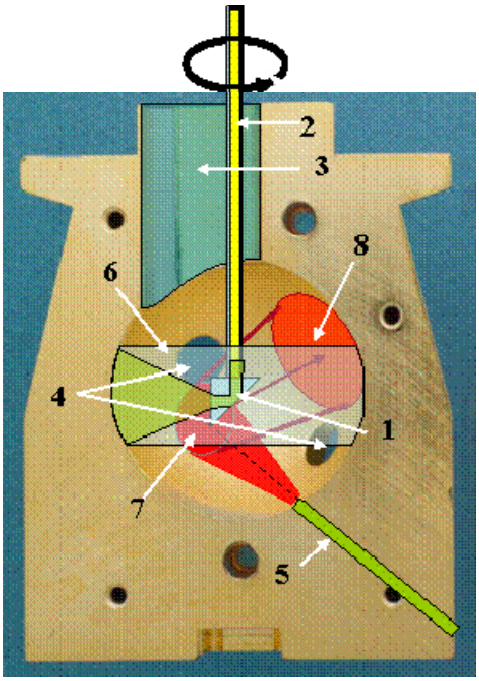

Fig. 3 Experimental setup of the periscope inside the layering sphere. 1: Periscope prism coupled to a 0.5mm optical fiber. 2: 0.5mm optical fiber through a rigid tube. 3: Keyhole. 4: Target viewing windows. 5: Fiber-coupled surrogate LED. 6: Schematic of the equatorial region "seen" by periscope. 7: First-bounce bright spot. 8: Second-bounce bright spot.

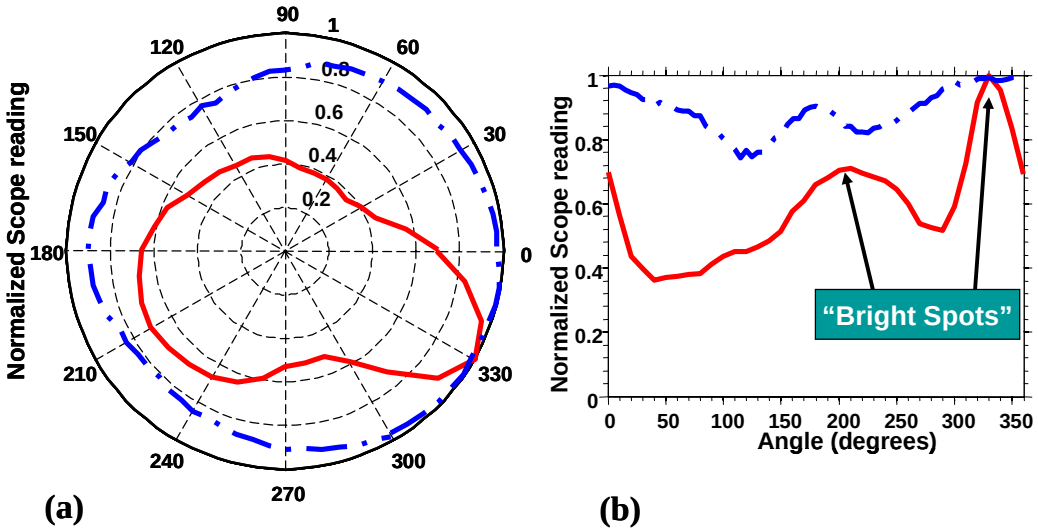

Fig. 4 Normalized intensity *versus* angle of periscope rotation in (a) polar and (b) Cartesian plot. Red curves (solid): the layering sphere with all windows closed. Blue curves (dash-dot): a perfect integrating sphere.

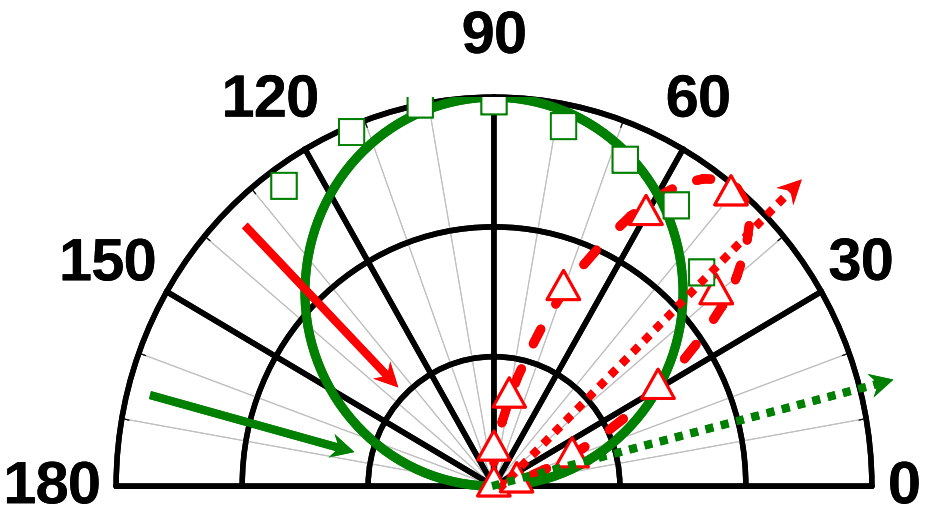

Fig. 5 Normalized reflected intensity *versus* angle (degree) in polar plot. Typical roughened, gold-coated surface - red arrow (solid): incident ray at 135°; red arrow (dotted): specular reflection at 45°; red (triangles): measured intensity distribution[9]; red curve (dash): calculated intensity distribution using $\cos^9(\theta-\theta_0)$ dependence[4]. Ideal surface of the witness piece to a perfect integrating sphere - green arrow (solid): incident green light (530nm) at 165°; green arrow (dotted): specular reflection at 15°; green (squares): measured intensity distribution; green curve (solid): calculated distribution using Lambert's cosine law.

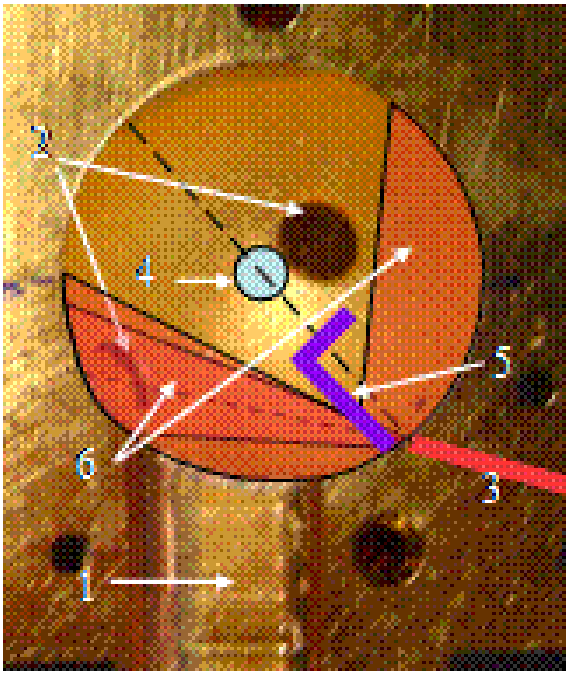

Fig. 6 Modified layering sphere with engineered diffuser mounted for optimal illumination uniformity at the center of the sphere. The components are 1: keyhole, 2: windows, 3: LED beam, 4: target location, 5: wide-angle diffuser configuration and 6: light spread by diffuser.

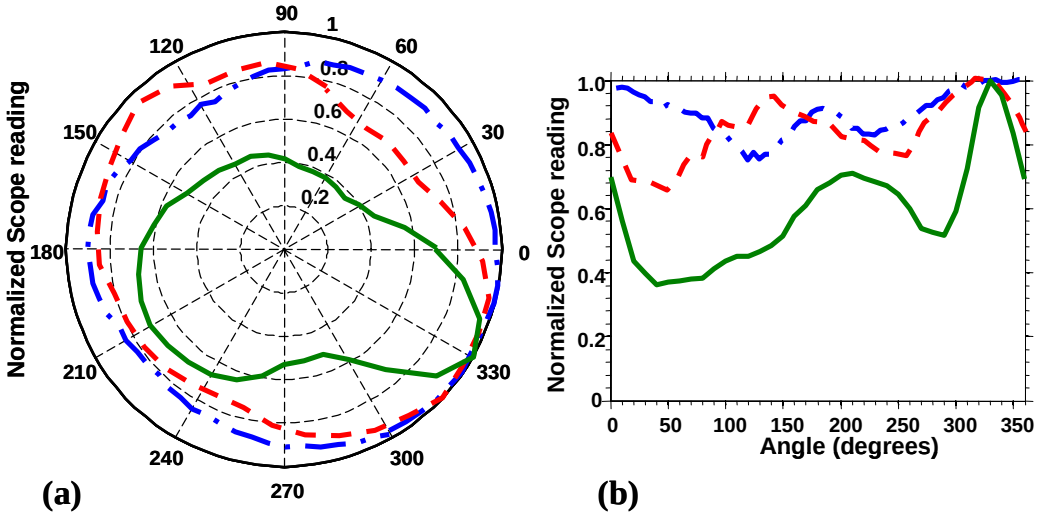

Fig. 7 Normalized intensity *versus* angle of periscope rotation in (a) polar plot and (b) Cartesian plot. Red curves (dash): layering sphere with the current best diffuser configuration. Green curves (solid): original layering sphere. Blue curves (dash-dot): a perfect integrating sphere.

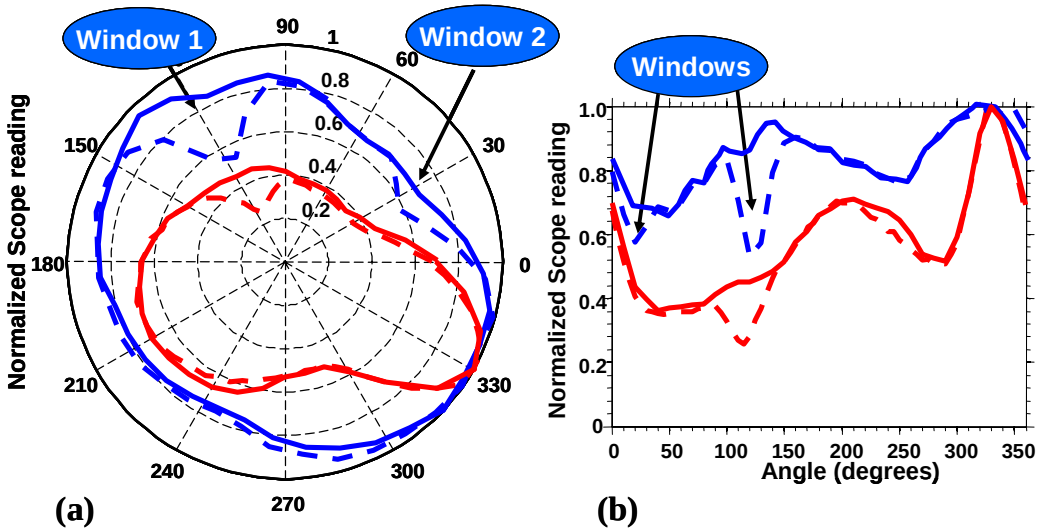

Fig. 8 Normalized intensity *versus* angle of periscope rotation in (a) polar plot and (b) Cartesian plot. Red curves: original layering sphere. Blue curves: modified layering sphere with the current best diffuser configuration. Solid curves: windows closed. Dash curves: windows open.

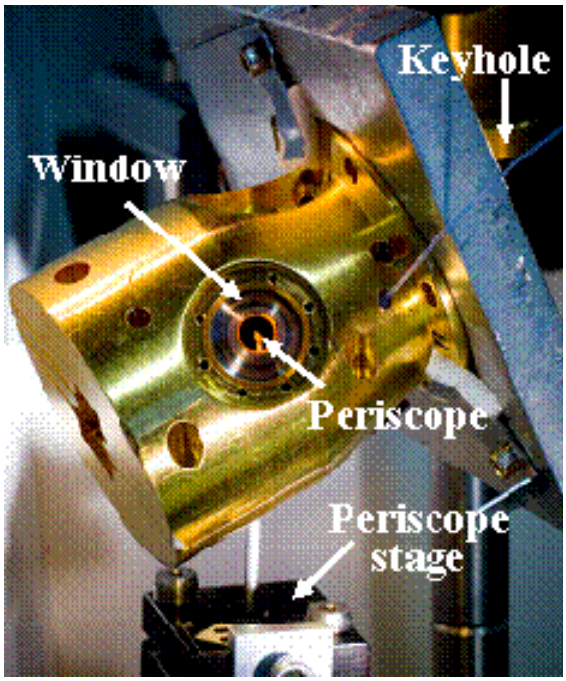

Fig. 9 Photograph of the tilted-view setup. The layering sphere is tilted and the periscope is inserted through a window.

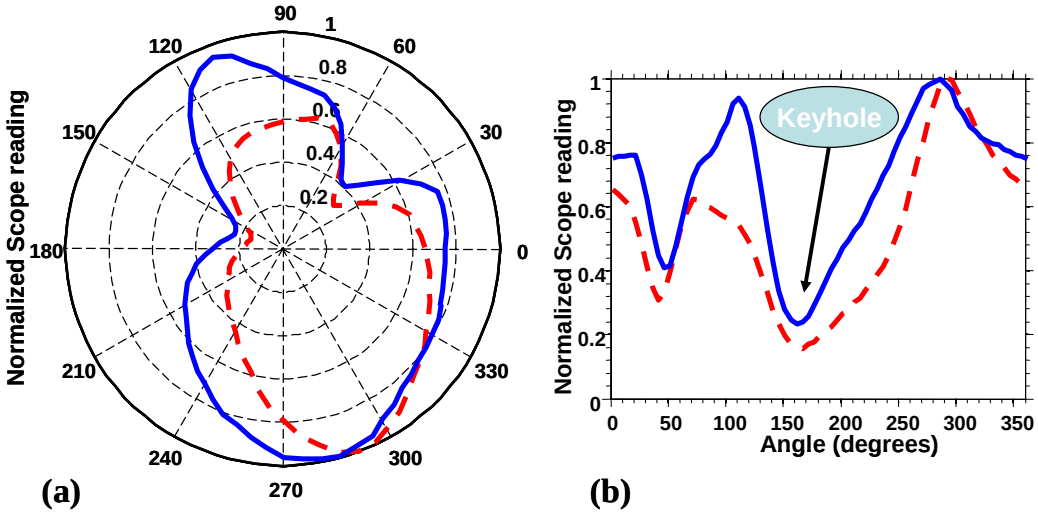

Fig. 10 Normalized intensity *versus* angle of periscope rotation in (a) polar plot and (b) Cartesian plot using the tilted-plan view. Blue curves (solid): the layering sphere modified with the current best diffuser configuration. Red curves (dash): the original layering sphere. Both with windows open.

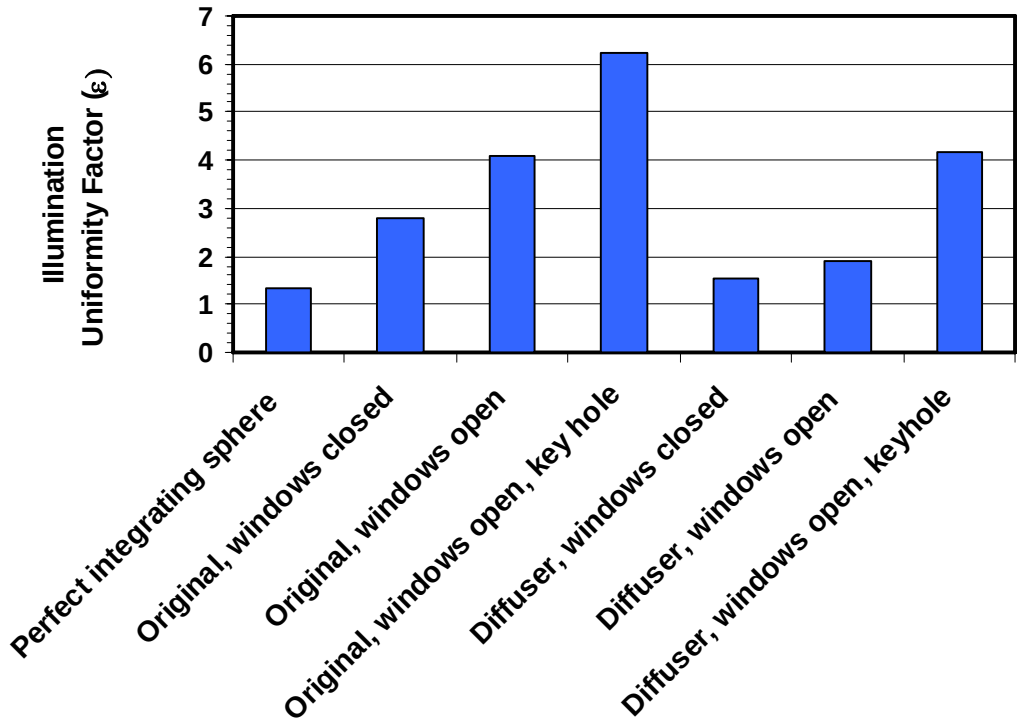

Fig. 11 Illumination uniformity factor *versus* different experimental settings.